SAGE-Hindawi Access to Research
International Journal of Alzheimer's Disease
Volume 2011, Article ID 607861, 7 pages
doi:10.4061/2011/607861

Research Article

Correlation of Copper Interaction, Copper-Driven Aggregation, and Copper-Driven H_2O_2 Formation with Aβ40 Conformation

Chia-Anne Yang,[1] Yung-Han Chen,[2] Shyue-Chu Ke,[2] Yi-Ru Chen,[3] Hsien-Bin Huang,[4] Ta-Hsien Lin,[5,6] and Yi-Cheng Chen[7]

[1] *Institute of Life Science, Tzu Chi University, Hualien 970, Taiwan*
[2] *Department of Physics, National Dong Hwa University, Hualien 974, Taiwan*
[3] *Institute of Pharmacology, National Yang-Ming University, Shihpai, Taipei 112, Taiwan*
[4] *Institute of Molecular Biology, National Chung-Cheng University, Chiayi 621, Taiwan*
[5] *Department of Biochemistry and Molecular Biology, National Yang-Ming University, Shihpai, Taipei 112, Taiwan*
[6] *Department of Medical Research & Education, Taipei Veterans General Hospital, Shihpai, Taipei 112, Taiwan*
[7] *Department of Medicine, Mackay Medical College, Taipei County 252, Taiwan*

Correspondence should be addressed to Ta-Hsien Lin, thlin@vghtpe.gov.tw and Yi-Cheng Chen, chen15@mmc.edu.tw

Received 15 September 2010; Accepted 15 November 2010

Academic Editor: Craig Atwood

The neurotoxicity of Aβ is associated with the formation of free radical by interacting with redox active metals such as Cu^{2+}. However, the relationship between ion-interaction, ion-driven free radical formation, and Aβ conformation remains to be further elucidated. In the present study, we investigated the correlation of Cu^{2+} interaction and Cu^{2+}-driven free radical formation with Aβ40 conformation. The Cu^{2+}-binding affinity for Aβ40 in random coiled form is 3-fold higher than that in stable helical form. Unexpectedly but interestingly, we demonstrate in the first time that the stable helical form of Aβ40 can induce the formation of H_2O_2 by interacting with Cu^{2+}. On the other hand, the H_2O_2 generation is repressed at Aβ/Cu^{2+} molar ratio ≥ 1 when Aβ40 adopts random coiled structure. Taken together, our result demonstrates that Aβ40 adopted a helical structure that may play a key factor for the formation of free radical with Cu^{2+} ions.

1. Introduction

β-Amyloid (Aβ) peptide is the main cause of Alzheimer's disease (AD) [1, 2]. Aβ has two major types, Aβ40 and Aβ42, which are derived from a ubiquitous type I transmembrane protein—amyloid precursor protein (APP) by a two-step secretase (β- and γ-secretase) pathway [3–5]. The amyloid cascade hypothesis predicts that the aggregated Aβ peptides in the brain have an early and essential role in the neuronal degeneration that leads to dementia [1, 2, 6]. The aggregation of Aβ occurs following a conformational conversion from either α-helix or random coil to β-sheet in a time-dependent manner, indicating that the formation of β-sheet structure is the key step for the peptide aggregation [7, 8].

The formation of Aβ aggregates is modulated by several factors, including metal ions [9, 10]. In amyloid plaques of AD-affected brain, remarkably high concentration of metals, such as Cu (400 μM), Zn (1 mM) and Fe (1 mM), has been found [11, 12]. *In vitro* studies, micromolar levels of Cu^{2+}, Zn^{2+} and Fe^{3+} have been shown to sufficiently induce protease-resistant aggregation and precipitation of Aβ [13]. Copper ions are bound to the three His residues of Aβ located at the N-terminus, which forms a 3N1O square-planar motif as verified by EPR spectroscopy [14]. Aβ/Cu^{2+} complexes have been demonstrated to generate neurotoxic H_2O_2 from O_2• through Cu^{2+} reduction [15]. Copper-selective chelators can dissolve Aβ deposits extracted from AD postmortem brain specimens and reduce the level of free radical [16].

Curtain and his colleagues previously reported that the addition of Cu^{2+} to oligomeric Aβ40 in a negatively charged lipid membrane can induce Aβ peptides reinserted into lipid membranes, convert Aβ conformation from β-strand into α-helix, and cause the lipid peroxidation [17]. Their result is the first study to show that instead of β-sheet, Aβ in α-helical

form can also generate free radicals in the presence of Cu ions. Recently, our group has characterized the conformation of Aβ in the presence of Cu ions into three structural states, stable helix, unstable helix, and random coil, in 40%, 25%, and 5% TFE, respectively, [18]. Therefore, this provides us a possibility to re-examine the relationship between Aβ conformation, and Cu-driven free radical generation.

In the present study, we examined the correlation between Cu^{2+} binding affinity, H_2O_2 formation, and Aβ40 conformation. It was found that both Cu^{2+} binding affinity and H_2O_2 formation are well correlated with the conformation of Aβ40. In general, Cu^{2+} ions can be bound to the different structural forms of Aβ40. The copper-binding affinity of Aβ40 in random coiled form is about 3-fold higher than that of Aβ40 in stable helical form. For H_2O_2 formation, our result shows in the first time that the generation of H_2O_2 can also be induced by Cu^{2+} and the stable helical form of Aβ40. In contrast, in random coiled form, the formation of H_2O_2 is inhibited by Aβ40.

2. Materials and Methods

2.1. Peptide Synthesis, Purification, and Sample Preparation. The synthesis of full-length Aβ40 peptide was performed in an ABI-433A solid-phase peptide synthesizer using the Fmoc protocol. Cleavage and deprotection of the synthesized peptide were performed by treatment with a mixture of trifluoroacetic acid/distilled water/phenol/thioanisole/ethanedithiol. Then the peptide was extracted with 1 : 1 (v : v) ether : H_2O containing 0.1% 2-mercaptoethanol. The synthesized Aβ peptides were purified on a reverse-phase C-18 HPLC with a linear gradient from 0% to 100% acetonitrile, and the molecular weight of Aβ40 peptides and purity was verified by an MALDI-TOF mass spectroscopy. One mg of purified monomeric Aβ40 peptide was dissolved in 1 mL 100% trifluoroethanol (TFE) as stock solution.

2.2. Circular Dichroism (CD) Spectroscopy. A final Aβ peptide concentration of 30 μM in either 5% or 40% TFE was prepared from fresh peptide stock solution diluted in phosphate buffer, pH 7.4, with or without the same concentration of Cu^{2+}. A thousand μM of Cu^{2+} stock solution was prepared by dissolved $CuCl_2$ salt in distilled H_2O purged by N_2 in a sealed flask and freshly diluted into the designed concentration before it was used. CD spectra were recorded using an Aviv spectropolarimeter equipped with a thermal circulator accessory. All measurements were performed in quartz cells with a path length of 0.1 cm. Data were collected at wavelengths from 190 to 260 nm in 0.2 nm increments. Every CD spectrum is reported as the average from at least three individual samples. The reported CD spectra were corrected using phosphate buffer, pH 7.4 for the baseline. All measurements were carried out at 25.0 ± 0.2°C.

2.3. Electron Paramagnetic Resonance (EPR) Spectroscopy. An equal molar 300 μM of Aβ and Cu^{2+} in 30% glycerol phosphate buffer, pH 7.4, and 5% and 40% of TFE was employed for spin counting purposes. EPR spectra were obtained at X-band using a Bruker EMX ER073 spectrometer equipped with a Bruker TE102 cavity and an advanced research system continuous-flow cryostat (4.2–300 K). During EPR experiments, the sample temperature was maintained at 10 K. The microwave frequency was measured with a Hewlett-Packard 5246L electronic counter.

2.4. Tyrosine Fluorescence Spectroscopy. Tyrosine fluorescence spectroscopy was used to investigate the binding affinity for copper bound to Aβ. Aβ peptide stock solution was diluted in phosphate buffer, pH 7.4 to a final peptide concentration of 10 μM with designed concentration of Cu^{2+}. All measurements were performed in a 96-well plate using a microplate reader (FlexStation 3, MD). The excitation and emission wavelengths were selected at 278 and 305 nm, respectively. Reported data were the average obtained from three individual samples and three repeated measurements of each sample.

The binding affinity was calculated using the following equation:

$$\frac{F_x}{F_0} = \frac{I_x - I_\infty}{I_0 - I_\infty} = \frac{1}{1 + K_a\left[\mathrm{Cu}^{2+}\right]^n}, \quad (1)$$

where I_0 and I_x are the fluorescence intensity for free and Aβ/Cu^{2+}complex, respectively, I_∞ is the fluorescence intensity at saturation state, $[Cu^{2+}]$ is the copper concentration, and n is the copper binding number. The related parameters were fitted using nonlinear curve fitting program MicroOrigin v6.0 (Microcal Software, Inc., Nothampton, MA). In the initial fitting stage, the simplex method, which was set to 100 cycle runs, was used to calculate the initial parameter for further nonlinear curve fitting. A 0.95 confidence level was set to constrain the quality of curve fitting. The final fitting parameters were obtained when the value of χ^2 was less than 0.05 and the parameters and errors for the parameters reached the convergent and steady state.

2.5. Hydrogen Peroxide Assay. The production of H_2O_2 was analyzed using the dichlorofluorescein diacetate (DCFH-DA) assay [19]. Dichlorofluorescein diacetate was dissolved in 100% dimethyl sulfoxide, deacetylated with 50% v/v 0.05 M NaOH for 30 min, and then neutralized (pH 7.4) to a final concentration of 200 μM as stock solution. This stock solution was kept on ice and in dark until use. The reactions were carried out in Dulbecco's PBS, pH 7.4, in a 96-well plate (100 μL/well) containing different concentration of Aβ40, 30 μM $CuCl_2$, TFE (5% and 40%), deacylated DCF (20 μM), and horseradish peroxidase (5 μM) at 37°C. For negative control, an extra of 1.0 mM catalase (*Aspergillus niger*) was used to quench H_2O_2. Measurements were performed on the day of sample preparation. Fluorescence readings were recorded on a microplate reader (MD, FlexStation 3), with the excitation and emission wavelengths selected at 485 and 530 nm, respectively.

2.6. Turbidity Assay. UV/Vis turbidity assay was used to detect the aggregation process of Aβ. 200 μL of 30 μM Aβ40

in phosphate buffer, pH 7.4 containing either 5% or 40% TFE was freshly prepared from stock solution. Fresh prepared samples with or without 30 μM Cu^{2+} placed in a 96-well plate were incubated at 37°C. Turbidity was measured using a microplate reader (MD, FlexStation 3) at a wavelength of 450 nm.

3. Results

The aim of this study is to examine the relationship between Aβ40 conformation and other physical and chemical properties such as aggregation, Cu-binding affinity, and free radical formation. In the present study, we applied 5% and 40% TFE to mimic the conformation of Aβ40 in random coil and stable helix, respectively, [18]. Therefore, the effect of TFE on Cu^{2+} binding affinity and free radical generation has to be evaluated. As depicted in supplemental data (see Supplementary Material available online at doi:10.4061/2011/607861), the main effect of TFE on the system is only to quench the DCF fluorescence intensity. Neither was the solubility of Cu^{2+} ions nor the formation of H_2O_2 affected by TFE.

3.1. Secondary Structure of Aβ40 and Aβ40/Cu^{2+}. First of all, we characterized the structural state of Aβ40 with and without Cu^{2+} in either 5% or 40% TFE using circular dichroism (CD) spectroscopy. Figures 1(a) and 1(b) show the CD spectra for Aβ40 and Aβ40/Cu^{2+} in 5% and 40% TFE, respectively. It can be seen that, in 5% TFE, the pattern of CD spectrum for Aβ40 in the presence of Cu^{2+} showed a dramatic change compared to that for Aβ40 only, while the CD spectra of Aβ40 with or without Cu^{2+} in 40% TFE did not show any significant change. The secondary structure of Aβ40 in 5% TFE changes from 63% random coil, 34% β-sheet and 3% helix in Cu^{2+}-free state to 45% random coil, 50% β-sheet and 5% helix in Cu^{2+}-bound state, representing that there is a structural conversion from random coil into β-sheet. On the other hand, the conformation of Aβ40 with or without Cu^{2+} in 40% TFE remains stable in which the secondary structure is 74% helix, 14% β-sheet, and 12% random coil in Cu^{2+}-free state and 73% helix, 15% β-sheet, and 12% random coil in Cu^{2+}-bound state, indicating that there is no conformational conversion of Aβ40 in 40% TFE while adding Cu^{2+} ions.

3.2. Correlation of Aggregation and Aβ40 Structure. It has been shown that Cu^{2+} ions are able to accelerate the aggregation of Aβ40 [9, 15, 18, 20]. Hence, we characterized the aggregation process of Aβ40/Cu^{2+} and Aβ40 in 5% and 40% TFE. The aggregation process of Aβ40/Cu^{2+} and Aβ40 in 5% and 40% TFE was analyzed by turbidity assay as shown in Figure 2. In general, in both 5% and 40% TFE, Aβ40 in the presence of Cu^{2+} was aggregated much faster than that in the absence of Cu^{2+}. Furthermore, the aggregation rate in 5% TFE for both Aβ40/Cu^{2+} and Aβ40 was much faster than that in 40% TFE. The aggregation process in 5% TFE for Aβ40/Cu^{2+} and Aβ40 showed a typical sigmoidal profile. On the other hand, the aggregation process in 40% TFE for Aβ40 with and without Cu^{2+} mostly stayed in the nucleation or the early elongating stage within 24 hrs. The aggregation process for Aβ40 and Aβ40/Cu^{2+} in 5% and 40% TFE echoes with the result obtained in the analyses of secondary structure in which the aggregation ability is correlated with the ability of conformational formation of β-sheet [8].

3.3. EPR Spectroscopy of Aβ40/Cu^{2+} in 5% and 40%. In the present study, we showed that the conformational states for Aβ40/Cu^{2+} and Aβ40 in 5% are dramatically different, while no such conformational change can be observed between Aβ40/Cu^{2+} and Aβ40 in 40% TFE. Although Cu^{2+} ions have been shown to be bound to Aβ in aqueous solution [14], then, whether Cu^{2+} ions are bound to Aβ40 in 40% TFE is needed to be investigated since the structural state for Aβ40/Cu^{2+} and Aβ40 in 40% TFE shows no difference. To address this issue, EPR spectroscopy was applied to explore the interaction between Cu^{2+} and Aβ40 in 40% TFE. As shown in Figure 3, the EPR spectra of Aβ/Cu^{2+} both in 5% and 40% TFE showed two major groups of hyperfine peaks, while no hyperfine peak could be observed in the EPR spectrum for Cu^{2+} alone, indicating that Cu^{2+} ions were bound to Aβ40 in both 5% and 40% TFE. The pattern of hyperfine peaks for Aβ40/Cu^{2+} in 5% and 40% TFE is similar, but the position of hyperfine peaks in 40% TFE shifts to low magnetic field. The related EPR parameters of $g_{\|}$, A, and $g_{\perp}$ are 2.28, 156.8, and 2.06 for Aβ40/Cu^{2+} in 5% TFE, respectively. The $g_{\|}$ and $g_{\perp}$ values in 5% TFE are very close to those in the literature measured in aqueous condition [14], representing that the binding geometry of Aβ40/Cu^{2+} in 5% TFE should adopt a similar 3N1O coordination. On the other hand, the related EPR parameters of $g_{\|}$, A, and $g_{\perp}$ are 2.40, 119.6, and 2.09 for Aβ40/Cu^{2+} in 40% TFE, indicating that the copper-binding geometry is different from the 3N1O mode and may be locally distorted in 40% TFE. Meanwhile, the A value in 5% TFE is larger than that in 40% TFE. This further indicates that the binding affinity of Cu^{2+} to Aβ40 in random coiled form may be stronger than that to Aβ40 in stable helical form.

3.4. Cu^{2+}-Binding Affinity in 5% and 40% TFE. As shown in EPR studies, Cu^{2+} can be bound to different structural forms of Aβ40 with a different binding affinity. In order to further elucidate the binding property of Cu^{2+}, we applied the tyrosine fluorescence spectroscopy to determine the Cu^{2+}-binding constant, since tyrosine 10 is the only fluorophore in Aβ amino acid sequence and locates at the binding pocket, in which the binding of $Cu^{2+}$to Aβ40 may cause the change of tyrosine fluorescence.

The titration curves of Cu^{2+} concentration versus tyrosine fluorescence intensity in 5% and 40% TFE are shown in Figures 4(a) and 4(b), respectively. The binding constants, K_a, were estimated using the equation as described in the experimental section with molar ratio of Aβ : Cu^{2+} = 1 : 1, that is, $n = 1$. The calculated K_a values are 0.14 μM^{-1} ($R^2 > 0.97$) and 0.05 μM^{-1} ($R^2 > 0.96$) for Aβ/Cu^{2+} in 5% and 40% TFE, respectively. The K_a of Aβ40/Cu^{2+} in 5% TFE is around 3-fold higher than that in 40% TFE, suggesting that Cu^{2+} is bound to random coiled form of Aβ40 more strongly than to

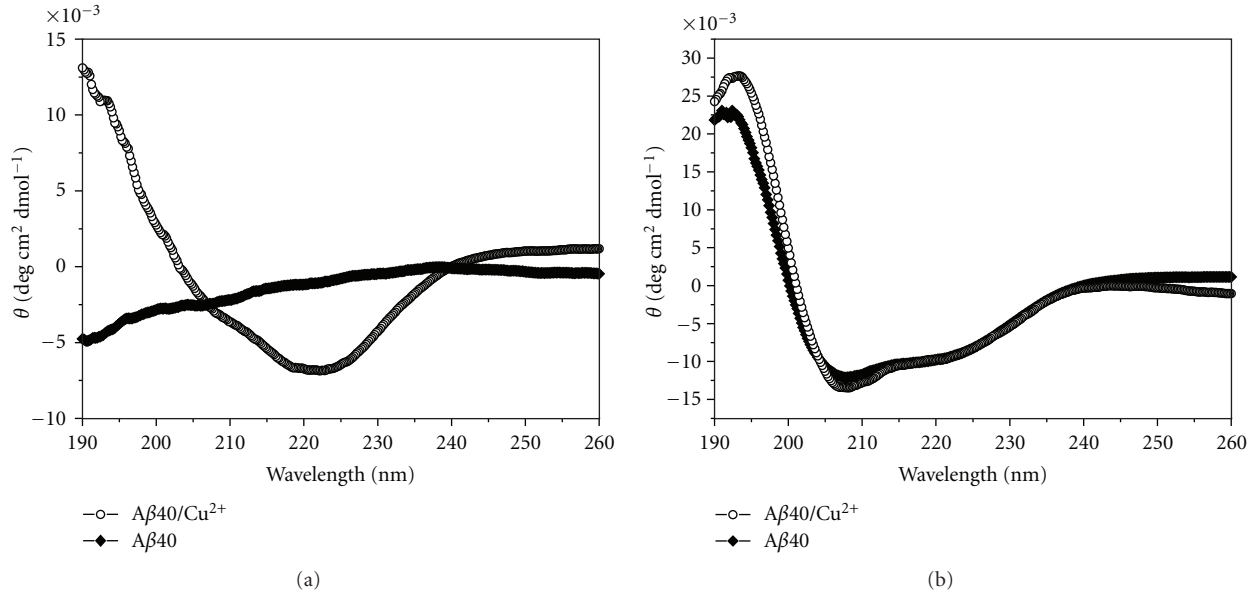

Figure 1: Circular dichroism spectra of Aβ40 peptide with or without Cu^{2+} in (a) 5% TFE and (b) 40% TFE. The concentration for both Aβ40 and Cu^{2+} used in measurements was 10 μM. It can be seen that the conformation of Aβ40 in 5% TFE shows a dramatic change in the presence of Cu^{2+}, while the conformation of Aβ40 in 40% TFE remains unchanged in the presence or absence of Cu^{2+}.

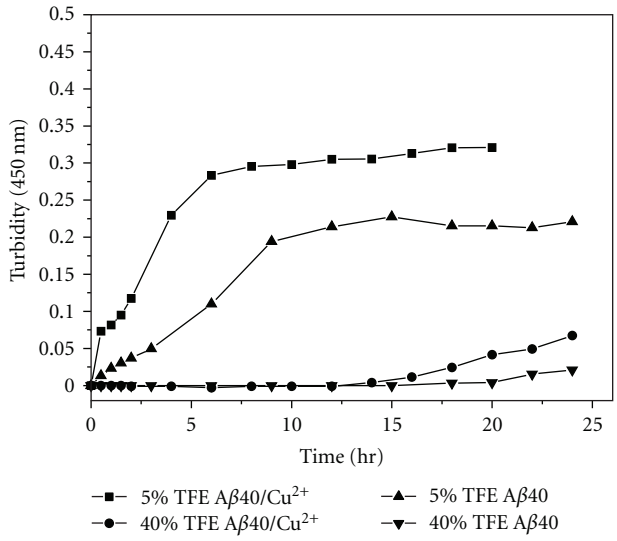

Figure 2: The aggregation process of Aβ40 and Aβ40/Cu^{2+} complex in 5% and 40% TFE measured by turbidity assay. (■) Aβ40/Cu^{2+} in 5% TFE, (▲) Aβ40 in 5% TFE, (•) Aβ40/Cu^{2+} in 40% TFE, and (▼) Aβ40 in 40% TFE.

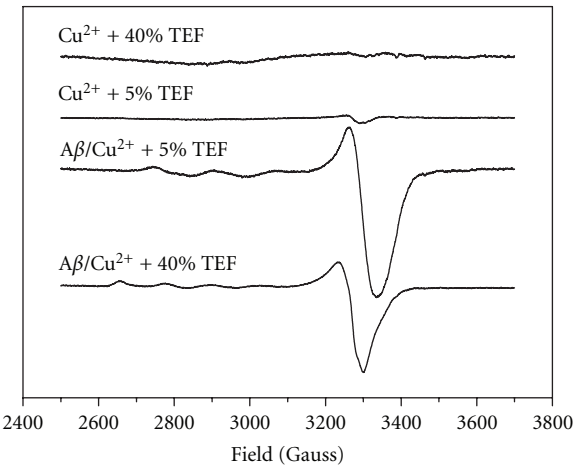

Figure 3: EPR spectra for Cu^{2+} only, Aβ40/Cu^{2+} in either 5% or 40% TFE. The characteristic $g_{\|}$ and $g_{\perp}$ hyperfine peaks appeared in 5% and 40% TFE represent that copper ion coordinates with Aβ40 in a 3N1O mode. The characteristic bands in 40% TFE are slightly shift downfield compared with the hyperfine peaks appeared in 5% TFE, suggesting that Aβ40 adopts different conformation in 5% and 40% TFE.

stable helical form of Aβ40 which is consistent with the EPR studies.

3.5. Hydrogen Peroxide Formation in 5% and 40% TFE. It has been demonstrated that Aβ40 coordinated with Cu^{2+} can cause the reduction of Cu^{2+} and then induce the formation of H_2O_2 from $O_2\cdot$ in a catalytic manner [15, 20]. To examine the relationship between free radical formation and Aβ40 conformation, DCF assay was used to detect the formation of H_2O_2. Figures 5(a) and 5(b) show the plots of DCF fluorescence intensity versus Aβ concentration in 5% and 40% TFE as incubated at 37°C for 1 hr.

In general, results clearly show that the formation of H_2O_2 is also correlated with Aβ40 conformation. In 5% TFE, the H_2O_2 level was decreased with an increase of Aβ40 concentration. The level of H_2O_2 was reduced to zero when

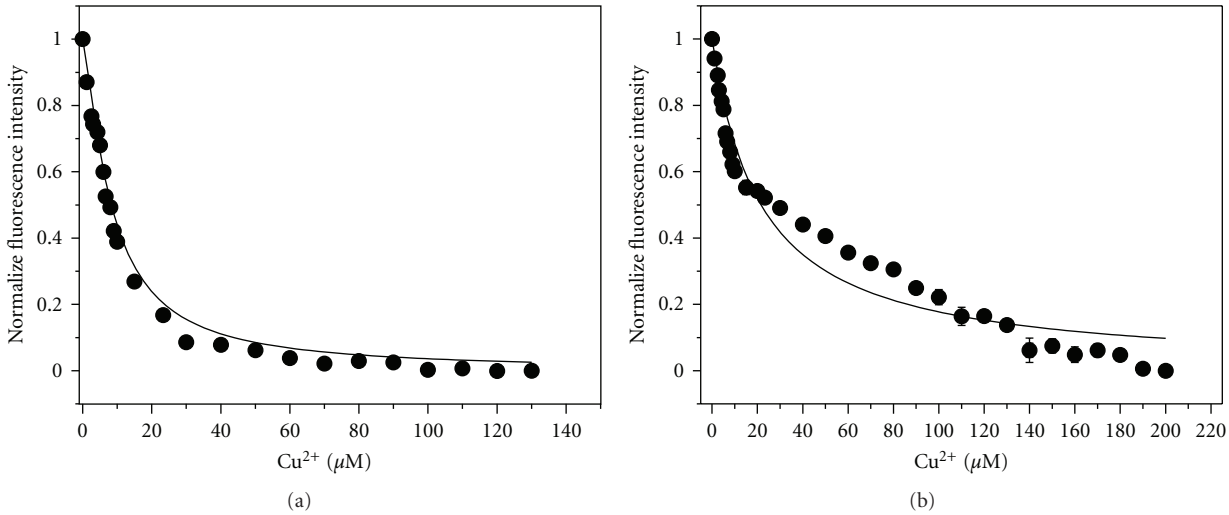

Figure 4: The binding affinity of Cu^{2+} to Aβ40 peptide in (a) 5% TFE and (b) 40% TFE measured by tyrosine fluorescence spectroscopy. Insets in (a) and (b) show the Jot plot. The concentration of Aβ40 was 10 μM. The solid lines represent the fitting curve using the equation as depicted in Section 2 with $n = 1$. The R^2 values in (a) and (b) are all >0.96, and the χ^2 values are <0.05.

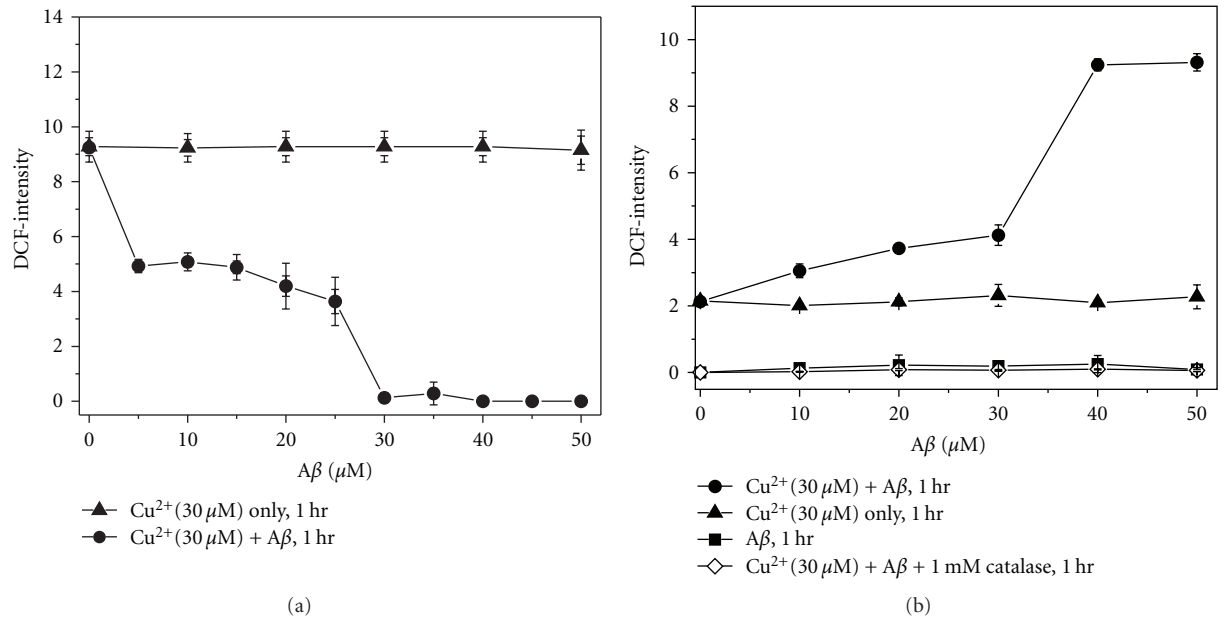

Figure 5: H_2O_2 generation assay for Aβ40 in (a) random coiled state (5% TFE) and (b) stable helical state (40% TFE). In (a), instead of generating free radicals, Aβ40 shows to inhibit the generation of free radical. (▲) 30 μM Cu^{2+} alone and (•) titration of Aβ40 with 30 μM Cu^{2+}. On the other hand, in stable helical structure (b), Aβ40 produces free radical with copper, in (▲) 30 μM Cu^{2+} alone, (■) Aβ40 alone, (•) titration of Aβ40 with 30 μM Cu^{2+}, and (◇) Aβ40 with 30 μM Cu^{2+} and 1 mM Catalase. All measurements were incubated at 37°C for 1 hour.

the Aβ40/Cu^{2+} molar ratio ≥1, indicating that the formation of H_2O_2 is inhibited when Aβ40 adopts the random coiled form. Unexpectedly but interestingly, unlike the formation of H_2O_2 which was inhibited in 5% TFE, the level of H_2O_2 in 40% TFE was increased with an increase of Aβ40 concentration and was much higher than those of either Cu^{2+} or Aβ40 alone, suggesting that the formation of H_2O_2 was induced when Aβ40 was in the stable helical form.

4. Discussion

According to amyloid cascade hypothesis, aggregated Aβ is the main toxic species to cause the Alzheimer's disease [6]. The various forms of Aβ aggregate have been shown to coordinate with redox active transition metals, such as Cu^{2+} and Fe^{3+}, and induce the generation of reactive oxygen species [15, 20]. However, the correlation of copper-binding

affinity, copper-driven aggregation, and free radical formation with Aβ40 conformation still needs to be elucidated.

For ion interaction, our results demonstrate for the first time that Cu^{2+} ions can interact with both random coiled and stable helical forms of Aβ40. As a larger A value and binding constant obtained for Aβ40 in 5% TFE, the Cu^{2+}-binding affinity for random coiled form of Aβ40 is much stronger than that for stable helical form of Aβ40. The possible explanation may be attributed to the different flexibility of Aβ40 conformation in 5% and 40% TFE. As shown in CD spectra, the conformation of Aβ40 in 5% TFE is relatively flexible and can easily convert structure from random coil into β-sheet while coordinating with Cu^{2+}. On the other hand, the overall conformation of Aβ40 with or without Cu^{2+} is relatively rigid and remains in stable helix in 40% TFE, and only the local geometry of Cu^{2+}-binding site is distorted while interacting with Cu^{2+} ions as indicated by the shift of $g_{\|}$ value. Therefore, the interaction between Cu^{2+} and Aβ40 is strong in 5% TFE and relatively weak in 40% TFE. The binding affinity for stable helical form of Aβ40 is almost 3-fold lower than that for random coiled form of Aβ40.

The Cu^{2+}-binding affinity can further be used to account for the differences for Cu^{2+}-driven aggregation between random coiled and stable helical forms of Aβ40. It is well known that the formation of β-sheet plays a key step for the aggregation of Aβ40 [8]. As shown in the present study, the conformation of Aβ40 in 5% TFE is much easier than that in 40% TFE to convert into β-strand structure by Cu^{2+} ions. Thus, in the presence of Cu^{2+}, the random coiled form of Aβ40 (in 5% TFE) aggregates faster and more severe than the stable helical form of Aβ40 (in 40% TFE).

Unlike the cascade hypothesis that only β-sheet form of aggregated Aβ can produce free radical, we demonstrate that helical form of Aβ40 can also induce the formation of H_2O_2. From the aggregation assay, this helical form of Aβ40 may possibly exist as a monomer during the early incubation period. Then, this further implies that monomeric Aβ40 in stable helical form by coordinating with Cu^{2+} can induce the formation of H_2O_2. In contrast, Aβ40 in random coiled form shows to inhibit the formation of H_2O_2 during the early incubation period. The inhibition of H_2O_2 formation becomes more significant with an increase of Aβ40 concentration, and the formation of H_2O_2 further is completely inhibited when the molar ratio of Aβ/Cu^{2+} molar ratio $\geq$1. Our observation is consistent with a recent study by Viles and his colleagues, in which they showed that, at Aβ/Cu^{2+} molar ratio =1, the formation of H_2O_2 is inhibited by both monomeric and fibrillar Aβ peptides [21]. Taken together, it may suggest that helical structure may play a key factor for the generation of H_2O_2 by Aβ40/Cu^{2+}.

In summary, our present results demonstrate that both ion interaction and copper-driven free radical formation are well correlated with Aβ40 conformation. When Aβ40 adopts a stable helical structure, the Cu^{2+} binding affinity is weaker, and the free radical is produced. On the other hand, when Aβ40 adopts a random coil in 5% TFE, the Cu^{2+} binding affinity is stronger, and the formation of H_2O_2 is inhibited.

Acknowledgments

This work was supported by Grants from the National Science Council of Taiwan, Taiwan (NSC 962113M320-001 and NSC 972627M320 to Y. C. Chen) and Taipei Veterans General Hospital, Taiwan, Republic of China (V97C1-036, V97S4-007 to T. H. Lin). C. A. Yang and Y. H. Chen contributed equally to the paper.

References

[1] D. J. Selkoe, "The molecular pathology of Alzheimer's disease," *Neuron*, vol. 6, no. 4, pp. 487–498, 1991.

[2] D. M. Skovronsky, R. W. Doms, and V. M. Y. Lee, "Detection of a novel intraneuronal pool of insoluble amyloid β protein that accumulates with time in culture," *Journal of Cell Biology*, vol. 141, no. 4, pp. 1031–1039, 1998.

[3] R. E. Tanzi, E. D. Bird, S. A. Latt, and R. L. Neve, "The amyloid β protein gene is not duplicated in brains from patients with Alzheimer's disease," *Science*, vol. 238, no. 4827, pp. 666–669, 1987.

[4] J. Kang, H.-G. Lemaire, and A. Unterbeck, "The precursor of Alzheimer's disease amyloid A4 protein resembles a cell-surface receptor," *Nature*, vol. 325, no. 6106, pp. 733–736, 1987.

[5] C. Haass, A. Y. Hung, M. G. Schlossmacher, D. B. Teplow, and D. J. Selkoe, "β-Amyloid peptide and a 3-kDa fragment are derived by distinct cellular mechanisms," *Journal of Biological Chemistry*, vol. 268, no. 5, pp. 3021–3024, 1993.

[6] E. Levy, M. D. Carman, I. J. Fernandez-Madrid et al., "Mutation of the Alzheimer's disease amyloid gene in hereditary cerebral hemorrhage, Dutch type," *Science*, vol. 248, no. 4959, pp. 1124–1126, 1990.

[7] A. Lomakin, D. S. Chung, G. B. Benedek, D. A. Kirschner, and D. B. Teplow, "On the nucleation and growth of amyloid β-protein fibrils: detection of nuclei and quantitation of rate constants," *Proceedings of the National Academy of Sciences of the United States of America*, vol. 93, no. 3, pp. 1125–1129, 1996.

[8] C. J. Barrow, A. Yasuda, P. T. M. Kenny, and M. G. Zagorski, "Solution conformations and aggregational properties of synthetic amyloid β-peptides of Alzheimer's disease: analysis of circular dichroism spectra," *Journal of Molecular Biology*, vol. 225, no. 4, pp. 1075–1093, 1992.

[9] C. S. Atwood, R. D. Moir, X. Huang et al., "Dramatic aggregation of alzheimer by Cu(II) is induced by conditions representing physiological acidosis," *Journal of Biological Chemistry*, vol. 273, no. 21, pp. 12817–12826, 1998.

[10] A. I. Bush, G. Multhaup, R. D. Moir et al., "A novel zinc(II) binding site modulates the function of the βA4 amyloid protein precursor of Alzheimer's disease," *Journal of Biological Chemistry*, vol. 268, no. 22, pp. 16109–16112, 1993.

[11] M. A. Lovell, J. D. Robertson, W. J. Teesdale, J. L. Campbell, and W. R. Markesbery, "Copper, iron and zinc in Alzheimer's disease senile plaques," *Journal of the Neurological Sciences*, vol. 158, no. 1, pp. 47–52, 1998.

[12] M. A. Smith, P. L. R. Harris, L. M. Sayre, and G. Perry, "Iron accumulation in Alzheimer disease is a source of redox-generated free radicals," *Proceedings of the National Academy of Sciences of the United States of America*, vol. 94, no. 18, pp. 9866–9868, 1997.

[13] W. Garzon-Rodriguez, M. Sepulveda-Becerra, S. Milton, and C. G. Glabe, "Soluble amyloid Aβ-(1-40) exists as a stable

dimer at low concentrations," *Journal of Biological Chemistry*, vol. 272, no. 34, pp. 21037–21044, 1997.

[14] C. D. Syme, R. C. Nadal, S. E. J. Rigby, and J. H. Viles, "Copper binding to the amyloid-β (aβ) peptide associated with Alzheimer's disease: folding, coordination geometry, pH dependence, stoichiometry, and affinity of Aβ-(1–28): insights from a range of complementary spectroscopic techniques," *Journal of Biological Chemistry*, vol. 279, no. 18, pp. 18169–18177, 2004.

[15] X. Huang, C. S. Atwood, M. A. Hartshorn et al., "The Aβ peptide of Alzheimer's disease directly produces hydrogen peroxide through metal ion reduction," *Biochemistry*, vol. 38, no. 24, pp. 7609–7616, 1999.

[16] R. A. Cherny, C. S. Atwood, M. E. Xilinas et al., "Treatment with a copper-zinc chelator markedly and rapidly inhibits β-amyloid accumulation in Alzheimer's disease transgenic mice," *Neuron*, vol. 30, no. 3, pp. 665–676, 2001.

[17] C. C. Curtain, F. Ali, I. Volitakis et al., "Alzheimer's disease amyloid-β binds copper and zinc to generate an allosterically ordered membrane-penetrating structure containing superoxide dismutase-like subunits," *Journal of Biological Chemistry*, vol. 276, no. 23, pp. 20466–20473, 2001.

[18] Y. R. Chen, H. B. Huang, C. L. Chyan, M. S. Shiao, T. H. Lin, and Y. C. Chen, "The effect of Aβ conformation on the metal affinity and aggregation mechanism studied by circular dichroism spectroscopy," *Journal of Biochemistry*, vol. 139, no. 4, pp. 733–740, 2006.

[19] C. Opazo, X. Huang, R. A. Cherny et al., "Metalloenzyme-like activity of Alzheimer's disease β-amyloid: cu-dependent catalytic conversion of dopamine, cholesterol, and biological reducing agents to neurotoxic HO," *Journal of Biological Chemistry*, vol. 277, no. 43, pp. 40302–40308, 2002.

[20] K. J. Barnham, F. Haeffner, G. D. Ciccotosto et al., "Tyrosine gated electron transfer is key to the toxic mechanism of Alzheimer's disease β-amyloid," *FASEB Journal*, vol. 18, no. 12, pp. 1427–1429, 2004.

[21] R. C. Nadal, S. E. J. Rigby, and J. H. Viles, "Amyloid β-Cu complexes in both monomeric and fibrillar forms do not generate HO catalytically but quench hydroxyl radicals," *Biochemistry*, vol. 47, no. 44, pp. 11653–11664, 2008.